AGU ADVANCING EARTH AND SPACE SCIENCES

Geophysical Research Letters

RESEARCH LETTER
10.1029/2025GL115747

Coeval Holocene Stalagmites Record Multi-Centennial Climate Variability and Drought in the Northern Rocky Mountains, USA

Bryce K. Belanger[1], Warren D. Sharp[2], Christopher W. Kinsley[2], Yanjun Cai[3], Cameron B. de Wet[4], Bryan L. McKenzie[5], and Jessica L. Oster[1]

[1]Department of Earth and Environmental Sciences, Vanderbilt University, Nashville, TN, USA, [2]Berkeley Geochronology Center, Berkeley, CA, USA, [3]Institute of Global Environmental Change, Xi'an Jiaotong University, Xi'an, China, [4]Department of Earth and Climate Sciences, Middlebury College, Middlebury, VT, USA, [5]US Bureau of Land Management, Cody Field Office, Cody, WY, USA

Key Points:

- Replicated Wyoming stalagmite proxy records are consistent with other records of Rocky Mountain winter precipitation
- Increased El Niño frequency coincides with aridity in the northern Rocky Mountains during the Holocene
- Multi-decadal north-south precipitation anomaly dipole patterns have occurred in the Rocky Mountains for at least the past 2800 years

Supporting Information:

Supporting Information may be found in the online version of this article.

Correspondence to:

B. K. Belanger,
bryce.k.belanger@vanderbilt.edu

Citation:

Belanger, B. K., Sharp, W. D., Kinsley, C. W., Cai, Y., de Wet, C. B., McKenzie, B. L., & Oster, J. L. (2025). Coeval Holocene stalagmites record multi-centennial climate variability and drought in the northern Rocky Mountains, USA. *Geophysical Research Letters*, *52*, e2025GL115747. https://doi.org/10.1029/2025GL115747

Received 12 MAR 2025
Accepted 26 AUG 2025

Author Contributions:

Conceptualization: Bryce K. Belanger, Warren D. Sharp, Christopher W. Kinsley, Cameron B. de Wet, Jessica L. Oster
Data curation: Bryce K. Belanger, Warren D. Sharp, Cameron B. de Wet, Jessica L. Oster
Formal analysis: Bryce K. Belanger, Warren D. Sharp, Christopher W. Kinsley, Yanjun Cai, Jessica L. Oster
Funding acquisition: Bryce K. Belanger, Warren D. Sharp, Jessica L. Oster
Investigation: Bryce K. Belanger, Warren D. Sharp, Christopher W. Kinsley, Yanjun Cai, Cameron B. de Wet, Bryan L. McKenzie, Jessica L. Oster

Abstract The El Niño Southern Oscillation and Pacific Decadal Oscillation (PDO) are key drivers of cool-season precipitation variability in the western United States (US), including the Rocky Mountains. Together, they help modulate the north-south "precipitation dipole," a regional climate pattern operating on multi-decadal timescales leading to dry conditions north of 40°N latitude when the south is wet, and vice versa. We investigate the natural evolution of this climate pattern using two precisely-dated (5900 years ago to present), multi-proxy, coeval stalagmite records of hydroclimate from Titan Cave, Wyoming, located just north of the modern-day dipole transition zone. Consistent trace element and stable isotope records from the two stalagmites reflect the amount and seasonality of regional precipitation, documenting decreased winter snowfall and dry conditions over multi-decadal intervals characterized by the warm phase of the PDO and more frequent and stronger El Niño events.

Plain Language Summary Pacific Ocean climate patterns such as the El Niño-Southern Oscillation have been shown to influence modern precipitation and drought in the western United States. Using analyses of carbonates formed in Titan Cave in northern Wyoming, we develop a record of how rain and snowfall in the northern Rockies have varied over the past 5900 years. We show that oscillating, centuries-long wet and dry periods extend thousands of years into the past and observe a persistent relationship between decreased snowfall in the northern Rockies and increased frequency of El Niño events.

1. Introduction

Defining patterns of precipitation change in the western United States (US) during the late Holocene and identifying key atmospheric teleconnections that drove them are fundamental to understanding regional climate and mitigating future climate risk (Cook et al., 2016). In the western US, modern winter precipitation anomalies often display a north-south/wet-dry "precipitation dipole" pattern, modulated by many factors including the El Niño Southern Oscillation (ENSO) and the Pacific Decadal Oscillation (PDO) (Wise, 2010). During concurrent warm phases of both patterns (PDO+ and El Niño) the northwestern US tends to experience a drier than average winter, and the southwestern US tends to experience a wetter than average winter. This pattern is inverted during concurrent cold phases (PDO- and La Niña) (Cole & Cook, 1998; Sung et al., 2014). The dipole pattern manifests due to shifts in the position of the North Pacific wintertime stormtrack as the result of PDO and ENSO teleconnections with the Aleutian Low (AL) (Alexander et al., 2002). These teleconnections are associated with N–S anomalies in snowpack (Pederson et al., 2011) and extreme precipitation events (Dettinger et al., 1998) in the western US during the last millennium.

Models suggest that fossil fuel-intensive future scenarios could lead to a stronger AL and more frequent south-shifted stormtracks across the western US on multi-decadal timescales (Giamalaki et al., 2021). Low-pressure extremes in the AL can produce strong high-pressure ridges over the Pacific Northwest (PNW), deflecting the stormtrack south following a more meridional flow (Wise, 2016). This south-shifted stormtrack would yield the dry-north/wet-south dipole pattern, a manifestation of the PDO+/El Niño scenario associated with sustained droughts in the northwestern US. Past multi-decadal droughts following this dipole pattern (Pederson et al., 2011) have had devastating effects on agriculture and human populations (Cook et al., 2007). Furthermore, models show

Methodology: Bryce K. Belanger, Warren D. Sharp, Christopher W. Kinsley, Yanjun Cai, Cameron B. de Wet, Jessica L. Oster
Project administration: Bryce K. Belanger, Jessica L. Oster
Resources: Bryce K. Belanger, Warren D. Sharp, Cameron B. de Wet, Bryan L. McKenzie, Jessica L. Oster
Supervision: Warren D. Sharp, Jessica L. Oster
Validation: Jessica L. Oster
Visualization: Bryce K. Belanger, Jessica L. Oster
Writing – original draft: Bryce K. Belanger, Warren D. Sharp, Christopher W. Kinsley, Cameron B. de Wet, Jessica L. Oster
Writing – review & editing: Bryce K. Belanger, Warren D. Sharp, Christopher W. Kinsley, Yanjun Cai, Cameron B. de Wet, Bryan L. McKenzie, Jessica L. Oster

future greenhouse warming may promote more frequent extreme El Niño events with >2°C equatorial Pacific SST anomalies (Thirumalai et al., 2024), which would also yield anomalously dry conditions in the northwestern US (Stone et al., 2023).

Our ability to ground-truth these hypothesized future scenarios using paleoclimate data has been limited by the extent of the tree ring record, which offers high temporal resolution but becomes increasingly sparse prior to 1000 CE (Pederson et al., 2011). Lake sediment records are longer-lived and provide foundational evidence for the timing of precipitation dipole initiation and persistence in the western US. Anti-phased variations in lake sediment δ^{18}O between sites in northern Canada and Colorado emerge at ∼4000 years BP (Anderson et al., 2016), coincident with stronger ENSO variability noted in lake sediment records from the Galápagos (Conroy et al., 2008) and Ecuador (Mark et al., 2022), a decreased Pacific Ocean zonal SST gradient (Koutavas et al., 2006), and warmer North Pacific SSTs (Praetorius et al., 2015). However, these lake records are geographically dispersed and are not proximal to the current dipole transition zone at ∼40°N latitude, limiting precise determination of spatial and temporal variations in past drought patterns.

We present multi-proxy stalagmite records of winter precipitation from Titan Cave (TC), located north of the present dipole boundary in northern Wyoming (WY). These include δ^{18}O, δ^{13}C, and trace element ratios (Mg/Ca, Sr/Ca, Ba/Ca, P/Ca) from stalagmites TC-2 and TC-7 that grew coevally over the past 2900 years with TC-2 extending to 5900 years BP. The new records allow us to assess the evolution of Holocene drought patterns in the western US and their relationship to ENSO and the PDO. We find strong correlations between TC stalagmite proxies and regional snowpack reconstructions, Pacific SSTs, and ENSO reconstructions and investigate the shifting nature of drought patterns via comparisons with sediment δ^{18}O records from lakes across the Rocky Mountains.

2. Methods

2.1. Site and Sample Description

TC is a wild cave developed in the Madison Limestone near the WY/Montana border in the Bighorn Basin (44.9°N, 108.2°W, 1427 m.a.s.l.) (Figure S1, Text S1 in Supporting Information S1). TC receives both cold-season precipitation (predominantly snow) and shoulder season/summer precipitation from convective storms (Bryson & Hare, 1974; Sjostrom et al., 2006). In spring and summer, the Atlantic Ocean and Gulf of Mexico can influence precipitation via the Great Plains Low Level Jet which delivers moisture from the south (Malloy & Kirtman, 2020). Snowfall is critical for water recharge at TC and likely dominates the annual precipitation budget as precipitation minus evaporation is highest in winter (Figure S2, Text S1 in Supporting Information S1). Given the importance of snowfall to recharge, our discussion focuses on winter precipitation variability, which is influenced by dynamics in the Pacific and the strength and position of the AL (Hunter et al., 2006; Stone et al., 2023). Winter bias in TC proxies is supported by measured TC drip water δ^{18}O values of −19.9 to −20.3‰ (VSMOW) (Belanger et al., 2024), which closely resemble estimated November-March precipitation δ^{18}O at TC (−20.6‰ VSMOW) (Bowen, 2025). While precipitation response to ENSO varies across the Rockies (Shinker & Bartlein, 2009; Wise, 2010), statistical analyses show winter precipitation in the Bighorn Basin is strongly correlated with ENSO variability. Preece et al. (2020) show significant drying during El Niño winters (DJF) at all elevations in the Bighorn Basin using both Kolmogorov-Smirnov and Ranked-Sum tests. Wetter conditions during La Niña winters are significant ($p < 0.05$) in Rank-Sum tests at the elevation of TC. Approximately 390 m above TC this La Niña winter precipitation increase is significant ($p < 0.01$) in both tests.

Stalagmites TC-7 (5 cm) and TC-2 (30 cm) were collected from the Pisa Room in 2019 and 2021, respectively (Figure S1 in Supporting Information S1). Each stalagmite was sliced in half vertically and subsamples for ^{230}Th/U dating were extracted from the growth axes in locations that were dense and free of silicate detritus using a hand-held dental drill. Thirteen subsamples from TC-2 were analyzed for ^{230}Th/U dating at the Berkeley Geochronology Center (BGC). From TC-7, 10 subsamples were analyzed at BGC and three were analyzed at the Institute of Global and Environmental Change, Xi'an Jiaotong University. Full descriptions of the cave, regional climate, and ^{230}Th/U dating procedures are provided in Supporting Information S1 (Text S2).

2.2. Trace Element and Stable Isotope Analysis

All trace element and stable isotope analyses were conducted at Vanderbilt University (Text S3 in Supporting Information S1). Trace element concentrations were measured along the growth axes of both stalagmites via laser ablation ICP-MS at ~20 μm spatial resolution. Samples for $\delta^{18}O$ and $\delta^{13}C$ analysis were milled along the growth axes of TC-2 and TC-7 at ~200 and ~100 μm spatial resolution, respectively. The $\delta^{18}O$ and $\delta^{13}C$ data are presented in per-mil (‰) relative to the international standard Vienna PeeDee Belemnite (VPDB). Spearman's rank and Pearson's correlation coefficients between TC proxies were calculated using cor.test() function in R (Table S1 in Supporting Information S1). Principal Component Analysis (PCA) and Empirical Orthogonal Function (EOF) analysis were conducted using the PCA() and prcomp() functions in R to compare TC proxies and investigate relationships with other Rocky Mountain records. The corit package in R is used to determine Pearson's correlation coefficients between TC and other records at specific timescales and compare these values with correlations produced using surrogate timeseries (Reschke et al., 2019) (Text S4 in Supporting Information S1).

3. Results and Discussion

3.1. Stalagmite Growth Histories

Dating results and calculated ages for TC-2 and TC-7 are listed in Tables S2 and S3 in Supporting Information S1. Median 2σ uncertainty of the calculated $^{230}Th/U$ ages is ±11.3 years for TC-2 and ±15.9 years for TC-7. TC-2 grew from 5732 ± 71 years BP to −14.4 ± 1.3 years BP (1964 CE) with a hiatus between 4024 ± 26 years BP and 2840 ± 24 years BP. The growth rate of TC-2 was ~0.005 mm/yr from the inception of growth to ~4000 years BP and increased to ~0.080 mm/yr after the hiatus until growth stopped around 1964 CE. TC-7 precipitated during the late Holocene, between 2851 ± 52 years BP and 54 ± 22 years BP (1896 CE) with a hiatus between 567 ± 32 years BP and 199.8 ± 5.8 years BP. TC-7 grew at ~0.004 mm/yr beginning approximately 2851 years BP until the hiatus, then at ~0.124 mm/yr after the hiatus until ~54 years BP.

Age-depth models were produced using the COPRA algorithm in Matlab (Breitenbach et al., 2012) (Figure S1 in Supporting Information S1). Based on similarities in the $\delta^{18}O$ records of the younger intervals of TC-7 and TC-2, we used tie-points with TC-2 $\delta^{18}O$ to refine the COPRA age-depth model for the older part of TC-7 (Figure S3, Text S2 in Supporting Information S1). We make these adjustments to account for offsets in $\delta^{18}O$ between stalagmites which likely manifest due to the extremely slow growth rate of TC-7 and comparatively large sample size required for $^{230}Th/U$ dating, making the age-depth model sensitive to uncertainty in sample depth.

3.2. Stalagmite Proxy Record Interpretations

The results of multi-year (2019–2024 CE) cave monitoring (Belanger et al., 2024) demonstrate that seasonal fluctuations in cave air temperature, relative humidity, and pCO_2 are minimal at TC. Mean cave temperature is 9.59°C ± 0.05°C, RH remains near 100%, and pCO_2 ranges from 469 to 654 ppm and is higher in fall and lower in spring. Drip rate and drip water isotopic composition show minimal responses to multi-annual regional precipitation trends: drip water $\delta^{18}O$ varied by less than 0.5‰ over a 2-year monitoring period (Belanger et al., 2024). Measured $\delta^{18}O$ and $\delta^{13}C$ of modern plate calcite are consistently lower in the center of the Pisa Room (location of TC-2) compared to the side (location of TC-7) by an average of 1.1‰ in $\delta^{18}O$ and 2.3‰ in $\delta^{13}C$. Notably, TC-2 $\delta^{18}O$ is 1–1.5‰ and $\delta^{13}C$ is 2.5–5‰ more negative than the respective isotope ratios in TC-7 (Figure 1), consistent with observations from modern plate calcite. The offsets in $\delta^{13}C$ and $\delta^{18}O$ suggest these proxies are differentially influenced by prior calcite precipitation (PCP), degassing, or isotopic exchange between cave air CO_2 and drip water bicarbonate before stalagmite precipitation. As the direction of these offsets are consistent through time and noted in both stalagmites and modern calcite, Rayleigh processes and carbon isotope exchange (CIE) are the most likely drivers (Parvez et al., 2024). Slower dripping at TC-7 allows increased time for CIE, driving $\delta^{13}C$ to more positive values reflective of the cave air (Skiba & Fohlmeister, 2023). Degassing of CO_2 can increase $\delta^{18}O$ at slower drip rates (Mickler et al., 2006). The $\delta^{13}C$ and $\delta^{18}O$ of TC-7 is more positive than TC-2 throughout the record, excluding the period of rapid TC-7 growth after ~1695 CE when drip rate likely increased significantly at TC-7. A positive $\delta^{18}O/\delta^{13}C$ slope of 0.2756 across all Pisa Room drip sites is consistent with disequilibria slopes reported in other caves likely influenced by CO_2 degassing/exchange processes (Belanger et al., 2024).

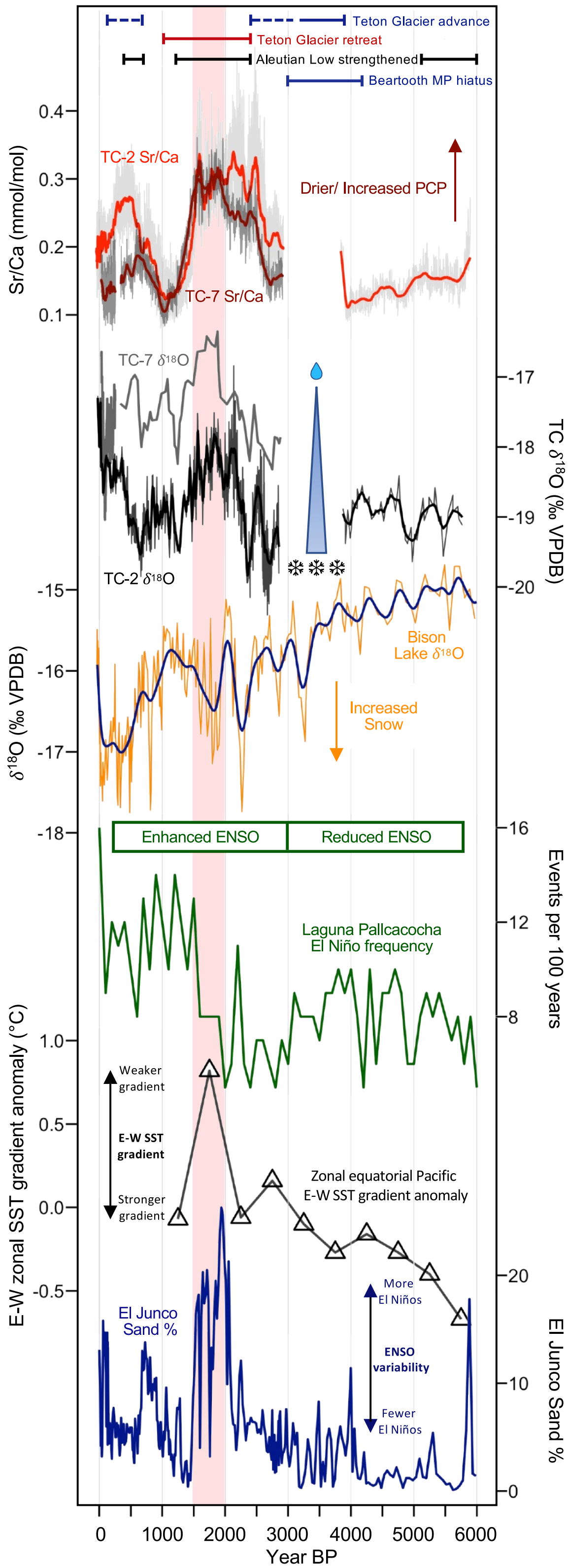

Figure 1. From top: Teton Glacier advance and retreat (Larsen et al., 2020), AL strengthening (Nagashima et al., 2021), Meltwater Pond hiatus (Alt et al., 2024), TC Sr/Ca, TC δ^{18}O, BL δ^{18}O (Anderson, 2011), El Niño frequency (Mark et al., 2022), Pacific SST gradient (Koutavas & Joanides, 2012), and El Junco Sand % (Conroy et al., 2008). "Enhanced" and "Reduced" El Niño Southern Oscillation for Laguna Pallcacocha as interpreted by original authors. For TC data, gray shading is raw data and bold line is COPRA mean. TC-7 δ^{18}O is raw data. Red shading from 2000 to 1500 years BP is interval of most frequent El Niños from Conroy et al. (2008).

The temporally consistent offsets between calcite precipitated in the center and sides of the Pisa Room, as well as the response of drip water stable isotopes to multi-year environmental changes, suggest that TC stalagmites record long-term climate variability. At similar inland western US sites, stalagmite δ^{18}O often reflects a combination of temperature, moisture source, and precipitation seasonality (Lachniet et al., 2014; Lundeen et al., 2013). At TC, δ^{18}O may reflect shifts in the seasonality of precipitation and relative contribution of snow versus rain, as snow-dominated intervals would yield lower δ^{18}O values. We interpret more negative δ^{18}O to reflect (a) colder winters, and (b) a greater contribution of snow versus rain to the annual moisture balance. A weakened AL can cause a more zonal, northward-shifted winter stormtrack and deliver increased moisture to the northern Rocky Mountains (Nagashima et al., 2021; Pederson et al., 2011; Woodhouse et al., 2009). Thus, negative stalagmite δ^{18}O is consistent with a weaker AL. Conversely, higher TC stalagmite δ^{18}O values likely reflect warmer winters, decreased snowfall, and a strengthened AL.

Trace element to calcium ratios in stalagmites are often interpreted to reflect PCP and water-rock interactions in the epikarst (Sinclair et al., 2012). Dry conditions lengthen water-rock contact times and increase the likelihood of CO_2 degassing, leading to elevated trace element ratios due to preferential exclusion of Sr, Mg, and Ba during $CaCO_3$ formation (Tremaine & Froelich, 2013). At TC, strong positive correlations between Sr/Ca and Ba/Ca (Table S1 in Supporting Information S1) and similar PCA loading suggest that these proxies are primarily influenced by PCP and reflect changes in water availability (Figure 1, Figures S4 and S5 in Supporting Information S1). Mg/Ca shows similar PCA loading in both stalagmites and strong positive correlations with Sr/Ca and Ba/Ca (Table S1 in Supporting Information S1), suggesting Mg/Ca is controlled at least in part by PCP processes. However, values are lower and display smaller amplitude variations in TC-2 than TC-7 indicating Mg/Ca is influenced by additional controls operating independently between the two drip sites (Figure S4 in Supporting Information S1). The presence of dolomite within the Madison Limestone (Barbier et al., 2015) and strong negative correlation and opposite PCA loading to P/Ca (Table S1, Figure S5 in Supporting Information S1) suggests that the differences in Mg/Ca between the two stalagmites may reflect variable dolomite contribution along different water flow paths. Stalagmite P/Ca, often interpreted to reflect variations in the amount of organic material flushed from the soil zone (Borsato et al., 2007; Oster et al., 2020), loads inversely on the PCA and is anti-correlated with Sr/Ca, Ba/Ca, and Mg/Ca in both stalagmites, suggesting more soil inputs during wetter intervals (Figures S4 and S5, Table S1 in Supporting Information S1). P/Ca increases during periods of faster stalagmite growth, consistent with increased water infiltration and delivery of soil-derived material to the drip site. This is highlighted by higher P/Ca ratios in the faster-growing TC-2 compared to TC-7. Enriched stalagmite δ^{13}C occurs simultaneously with periods of increased PCP recorded by Sr/Ca, Mg/Ca, and Ba/Ca, suggesting δ^{13}C is primarily controlled by water availability

(Figures S4 and S5, Table S1 in Supporting Information S1). Aridity can lead to decreased soil respiration and enhanced degassing of CO_2 from the drip water which favors the preferential removal of ^{12}C (Ersek et al., 2012; Oster et al., 2012, 2020). Above-cave vegetation (Burns et al., 2016), temperature (Fohlmeister et al., 2020), and atmospheric CO_2 concentrations (Breecker, 2017) may influence $\delta^{13}C$, but these are unlikely influences at TC over the Holocene.

Overall, TC $\delta^{13}C$ and trace elements indicate aridity during intervals when $\delta^{18}O$ suggests a rain-dominated precipitation balance. Likewise, when stalagmite $\delta^{18}O$ indicates more snow, PCP proxies indicate wetter conditions. Thus, TC stalagmites record changes in precipitation amount and the relative contribution of snow versus rain to annual precipitation in the Bighorn region.

3.3. Holocene Rocky Mountain Climate

The youngest, rapidly growing section of TC-7 formed from 1695 to 1920 CE and is sampled at monthly resolution for trace elements and near-annual resolution for stable isotopes, providing an excellent opportunity to examine multi-annual to centennial-scale climate variability. By comparison, the TC-2 record is longer but lower resolution (seasonal trace element resolution, ∼5-year stable isotope resolution). Thus, in the following sections, we use the TC-7 record to examine recent climate change at TC. We then use the TC-2 record (5897 to −47 years BP) to evaluate longer-term climate variations in the northern Rocky Mountains and compare with records from the western US and tropical Pacific.

3.3.1. Regional Climate Comparisons Over the Past ~300 Years

From 1695 to 1920 CE, TC-7 $\delta^{18}O$ exhibits moderate to strong correlations with Gulf of Alaska (GoA) SSTs (Wilson et al., 2007), the PDO Index (PDOI; D'Arrigo et al., 2001) reconstructed via a tree-ring network circling the GoA, and April 1 snow water equivalent (SWE) reconstructed via tree rings in the Bighorn region (Pederson et al., 2011) (Figure 2, Table S1 in Supporting Information S1). Strong correlations with Bighorn SWE suggest that TC proxies closely follow multi-annual variations in regional snowpack. As inferred from the northern Rocky Mountain tree ring record (Pederson et al., 2011), positive correlations between TC-7 proxies, GoA SSTs, and PDOI suggest a linkage between precipitation amount at TC and North Pacific climate, with winter precipitation in the northern Rockies increasing with negative PDOI and decreasing GoA SSTs. The similarities between TC-2 and TC-7 proxies alongside the robust relationships between TC-7 proxies and recent tree ring records suggests that TC-2 proxies reflect similar regional and global teleconnections during the mid-to late-Holocene.

3.3.2. Mid-to Early Late Holocene (5,900–2,900 Years BP)

Relatively low Sr/Ca, Ba/Ca, and Mg/Ca in TC-2 suggest limited PCP and wet conditions from ∼5900 to 3900 years BP. This is supported by elevated P/Ca and lower $\delta^{13}C$. Regionally, lake levels rise after ∼6000 years BP across northern WY (Alt et al., 2024; Pribyl & Shuman, 2014; Shuman & Serravezza, 2017) and the PNW (Lehmann et al., 2021; Mark et al., 2024), suggesting TC stalagmite growth occurred during a wetter, snowier interval. While TC-2 $\delta^{18}O$ is low, sediment $\delta^{18}O$ from Bison Lake (BL), central Colorado is near maximum values (Figure 1). Like TC, BL $\delta^{18}O$ is interpreted to reflect both winter temperature and precipitation seasonality, with more negative values indicating increased winter precipitation (Anderson et al., 2016). This north-south $\delta^{18}O$ contrast suggests wetter conditions at TC and drier conditions at BL and may indicate overall La Niña-like conditions and a generally north-shifted stormtrack from ∼5900 to 4000 years BP. The precipitation dipole may have been established during the mid-Holocene but with greatly reduced multidecadal variability compared to the late Holocene (Mark et al., 2024). Barron and Anderson (2011) note suppressed ENSO variability yet an overall La Niña-like state at this time, which would produce wetter winters in the northern Rockies.

TC-2 exhibits a hiatus bounded by ^{230}Th-U ages at 4024 ± 26 years BP and 2840 ± 24 years BP. While stalagmite hiatuses often reflect droughts or flow path changes, previous investigations of Rocky Mountain stalagmites suggest colder and/or wet conditions can freeze soil, inhibiting infiltration (Ersek et al., 2012; Lundeen et al., 2013). Current monitoring shows that soil temperatures above TC at 40 cm depth reach −4°C. Therefore, modest temperature depressions during the Holocene, combined with increased snowpack, may have been sufficient to temporarily halt stalagmite formation. Other northern WY proxies indicate cold, snowy conditions at this time. At ∼3900 years BP Teton Glacier began a major advance (Larsen et al., 2020), while Beartooth Ice Patch records more negative $\delta^{18}O$ values and doubled accretion rates (Chellman et al., 2021). The Beartooth

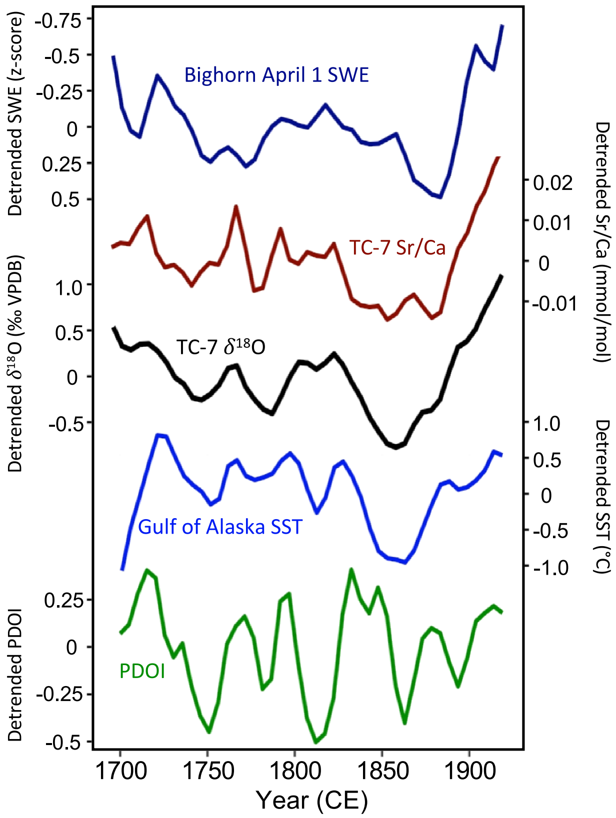

Figure 2. TC-7 $\delta^{18}O$ and Sr/Ca and relevant coeval climate records detrended and re-sampled to 5-year resolution (1695–1920 CE).

Meltwater Pond records a hiatus between 4200 and 3000 years BP, attributed to ice covering the pond for extended periods (Alt et al., 2024). Alternatively, this hiatus may suggest aridity at TC, consistent with lake records to the south which record drier conditions (Liefert & Shuman, 2022; Shuman et al., 2015). Water levels at Lake of the Woods (northern WY) are low from 4000 to 3000 years BP, rising concurrently with the re-initiation of speleothem growth at TC approximately 3000 years BP (Pribyl & Shuman, 2014). Based on the available information we are unable to determine which scenario led to this hiatus, however both highlight the intricacies of Rocky Mountain hydroclimate and support the idea that simple dipole drought patterns do not always dominate regional precipitation response.

3.3.3. Coeval Stalagmite Growth (2900–50 Years BP)

TC-2 and TC-7 proxies suggest wet, snow-dominated conditions as stalagmite growth is re-initiated after ~2,900 years BP (Figure 1). By ~2550 years BP, increases in $\delta^{18}O$ and PCP-sensitive proxies suggest drier conditions and decreased snowfall. Teton Glacier retreats ~2400 years BP (Figure 1) (Larsen et al., 2020), and Beartooth Ice Patch accretion rates drop (Chellman et al., 2021) consistent with decreased snowfall across the northern Rockies. Concurrently, BL $\delta^{18}O$ decreases, and EOF analysis shows anti-phased anomalies in $\delta^{18}O$ records across the ~40°N dipole boundary (Figure 1, Figure S6 in Supporting Information S1). We interpret intervals of opposing trends in TC and BL $\delta^{18}O$ to reflect migration of the stormtrack between more northern (lower $\delta^{18}O$ at TC, higher $\delta^{18}O$ at BL) or southern (higher $\delta^{18}O$ at TC, lower $\delta^{18}O$ at BL) positions in response to shifts in ENSO and the PDO which influence the strength and position of the AL (Giamalaki et al., 2021). A PDO + pattern and El Niño-like SSTs in the tropical Pacific strengthen the AL, driving a more southerly stormtrack that delivers increased winter moisture to the Rocky Mountains south of ~40°N. Conversely, a negative PDO, La Niña-like conditions, and a weakened AL shift the stormtrack north, increasing moisture north of ~40°N (Figure S7 in Supporting Information S1) (Pederson et al., 2011; Sung et al., 2014). When one ENSO/PDO pattern dominates on multi-decadal to multi-centennial timescales, the precipitation anomaly dipole observed in Figure 3 is produced.

These opposing precipitation patterns between TC and BL are first evident beginning ~2800–2550 years BP when decreased $\delta^{18}O$ at TC and increased $\delta^{18}O$ at BL suggest a north-shifted stormtrack (Figure 1). These observations are consistent with the N–S dipole pattern and suggest a weakened AL, negative PDO phase, and more zonal westerly flow, possibly marking the onset of modern tropical teleconnections with western US climate (Anderson et al., 2016; Carré et al., 2014). Strong negative correlations in $\delta^{18}O$ between TC in the north and both BL and Emerald Lake (Anderson et al., 2023) in the south are robust on multiple timescales of variation beginning 2200 years BP, indicating the dipole pattern is well-developed by this time (Figure S8 in Supporting Information S1).

After ~2,100 years BP the frequency of El Niño events increases (Fisler & Hendy, 2008; Mark et al., 2022) reaching maximum frequency and intensity between 2000 and 1500 years BP (Conroy et al., 2008). During this time proxies suggest sustained aridity at TC and wetter, snowier winters at BL (Anderson et al., 2016). This pattern is indicative of a south-shifted stormtrack, similar to current observations as El Niño winters are correlated with wetter winters in the southern US and increased aridity in the northern US (Sung et al., 2014; Wise, 2016).

After ~1500 years BP TC proxies record a trend toward wetter and snowier conditions and EOF analysis shows anti-phasing across the 40°N dipole boundary (Figure 3). The wettest interval of the TC record at ~1,100 years BP, synchronous with the end of Teton glacial retreat (Larsen et al., 2020), is consistent with La Niña-like conditions and a north-shifted stormtrack. This La Niña-like pattern continues through the beginning of the Medieval Climate Anomaly (MCA; 1150–650 years BP) as BL $\delta^{18}O$ is elevated and anti-phased with TC and Crevice Lake $\delta^{18}O$ (Figures 1 and 3). La Niña-like conditions are recorded by lake and pollen records in the

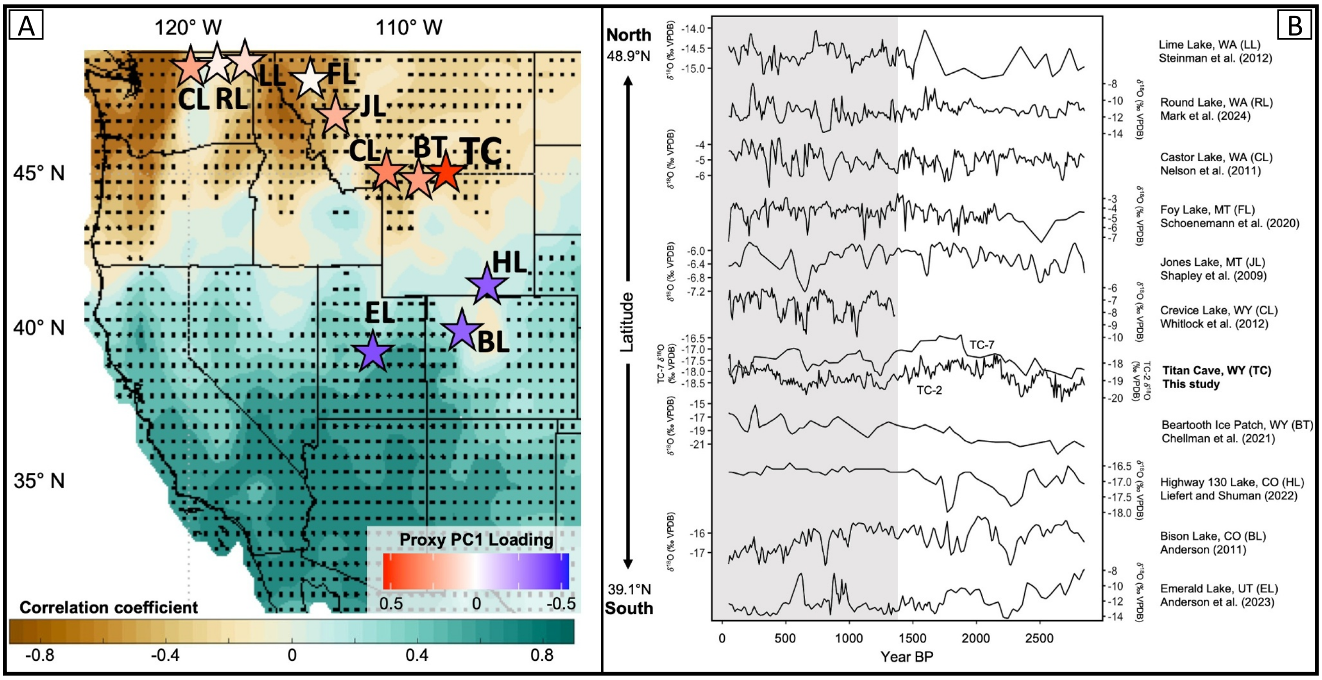

Figure 3. (a) Map of western United States adapted from Stone et al. (2023) showing the first mode of coupled variability between Pacific Ocean SSTs (10°S–70°N) and winter (DJFM) precipitation. Stippling indicates correlations significant at the 95% confidence level. Shading of star symbols shows PC1 loading of regional $\delta^{18}O$ records covering 1370–50 years BP (gray shading in B). See Figure S6 in Supporting Information S1 for PC1 loading for full record (2900–50 years BP). (b) Regional $\delta^{18}O$ records re-sampled to 10-year resolution over interval of overlap using prcomp() function in R.

western US (Jimenez-Moreno et al., 2021; Ladd et al., 2018; Shuman et al., 2018; Steinman et al., 2012, 2014) and records from both sides of the tropical Pacific suggest more frequent La Niña events during the MCA (Mark et al., 2022; Rodysill et al., 2019). However, a notable negative $\delta^{18}O$ excursion is recorded at BL at ~800 years BP. This climate shift supports the hypothesis that a single mode of Pacific Ocean-atmosphere forcing did not dominate during the entirety of the MCA (Anderson et al., 2016). However, we find that climate dynamics associated with an overall La Niña-like state likely promoted wetter winters in the northern Rockies during the MCA (Steinman et al. (2012, 2014).

The end of the MCA, after ~700 years BP, is also marked by opposing $\delta^{18}O$ trends at BL and TC suggesting a strengthened AL and south-shifted stormtrack, coincident with Alaskan lake and ice core records documenting AL intensification from 700 to 400 years BP (Figure 1) (Nagashima et al., 2021). We note drier winters during the first half of the Little Ice Age (LIA; 400–100 years BP) at TC in agreement with PNW records of aridity and El Niño-like conditions (Steinman et al., 2012, 2014). However, by ~1850 CE cold and snowy winters dominated at TC and the northern Rockies (Pederson et al., 2011). PCP-sensitive proxies decrease in both TC stalagmites, suggesting wetter conditions. Tree rings suggest high snowpack in the northern Rocky Mountains from 300 to 350 years BP (1650–1900 CE) (Pederson et al., 2011) including a "decadal-scale high snowpack anomaly" from ~1845 to 1895 CE, coinciding with the most negative $\delta^{18}O$ values of the TC-7 record (Figure 2) (~1860 CE). While the precipitation dipole may persist at this time, proxies across the Rockies record colder temperatures during the LIA (Anderson et al., 2016; Pederson et al., 2011). Beginning in 1890 CE, TC $\delta^{13}C$ and $\delta^{18}O$ increase to near-maximum values before growth stops in the 1900s CE, suggesting winter precipitation amounts in the mid to late 20th century were the lowest in this region since the mid-Holocene.

4. Conclusions

New TC stalagmite records are highly correlated with tree-ring based hydroclimate reconstructions during the last millennium and extend high-resolution records of past climate change in the northern Rocky Mountains to the mid-Holocene. Anti-correlation between $\delta^{18}O$ records from TC (44.9°N latitude) and BL (39.8°N latitude) along with other southern Rocky Mountain records suggests that the boundary of the western US dipole has remained near 40°N since at least ~2800 years BP. Correlations between TC stalagmite proxies and records of ENSO activity from the tropical Pacific indicate that El Niño events are linked to wintertime aridity in the northern Rocky Mountains during the late Holocene. Combined PDO+/El Niño can intensify the AL (Sung et al., 2014), driving more frequent south-shifted stormtracks that result in the dry-north/wet-south dipole pattern. If future El Niño and AL extremes increase as predicted (Giamalaki et al., 2021; Thirumalai et al., 2024), this may lead to more frequent, intense, and lengthened cold-season droughts in the northern Rocky Mountains.

Conflict of Interest

The authors declare no conflicts of interest relevant to this study.

Data Availability Statement

All TC-2 and TC-7 stalagmite chronology, trace element, and stable isotope data are available in the NOAA Paleoclimatology Data repository (https://www.ncei.noaa.gov/access/paleo-search/study/41479). Titan Cave monitoring data are available in Belanger et al. (2024).

Acknowledgments

This work was supported by NSF Grants AGS2102884 to JLO and AGS2102885 to WDS and a Vanderbilt Alberstadt-Reesman-Stearns award to JLO. BKB acknowledges support from GSA Graduate Student Research Grant 13028-21 and the Cave Research Foundation Graduate Research Grant. WDS and CWK thank Brian Jones for help with U-Th measurements. We thank Lisa Marks (Bureau of Land Management) and Aida Zyba (Vanderbilt University) for field assistance. We thank Richard Bradshaw for assistance with laboratory analyses.

References

Alexander, M. A., Bladé, I., Newman, M., Lanzante, J. R., Lau, N. C., & Scott, J. D. (2002). The atmospheric bridge: The influence of ENSO teleconnections on air–sea interaction over the global oceans. *Journal of Climate*, *15*(16), 2205–2231. https://doi.org/10.1175/1520-0442(2002)015<2205:TABTIO>2.0.CO;2

Alt, M., Puseman, K., Lee, C. M., Pederson, G. T., McConnell, J. R., Chellman, N. J., & McWethy, D. B. (2024). Organic layers preserved in ice patches: A new record of Holocene environmental change on the Beartooth Plateau, USA. *The Holocene*, *34*(3), 338–352. https://doi.org/10.1177/09596836231211877

Anderson, L. (2011). Holocene record of precipitation seasonality from lake calcite δ18O in the central rocky Mountains, United States. *Geology*, *39*(3), 211–214. https://doi.org/10.1130/G31575.1

Anderson, L., Berkelhammer, M., Barron, J. A., Steinman, B. A., Finney, B. P., & Abbott, M. B. (2016). Lake oxygen isotopes as recorders of north American rocky Mountain hydroclimate: Holocene patterns and variability at multi-decadal to millennial time scales. *Global and Planetary Change*, *137*, 131–148. https://doi.org/10.1016/j.gloplacha.2015.12.021

Anderson, L., Skipp, G., Strickland, L., Honke, J., Havens, J., & VanSistine, D. P. (2023). Holocene paleohydrology from alpine lake sediment, Emerald Lake, Wasatch Plateau of central Utah, USA. *Quaternary Research*, *112*, 1–19. https://doi.org/10.1017/qua.2022.42

Barbier, M., Floquet, M., Hamon, Y., & Callot, J. P. (2015). Nature and distribution of diagenetic phases and petrophysical properties of carbonates: The Mississippian Madison formation (Bighorn Basin, Wyoming, USA). *Marine and Petroleum Geology*, *67*, 230–248. https://doi.org/10.1016/j.marpetgeo.2015.05.026

Barron, J. A., & Anderson, L. (2011). Enhanced late Holocene ENSO/PDO expression along the margins of the eastern North Pacific. *Quaternary International*, *235*(1–2), 3–12. https://doi.org/10.1016/j.quaint.2010.02.026

Belanger, B., de Wet, C., McKenzie, B., & Oster, J. (2024). Modern cave monitoring informs interpretations of past climate change: Applications to Titan Cave, Wyoming. In *Reviewed conference proceedings for 2024 USGS karst interest group*. https://doi.org/10.3133/ofr20241067

Borsato, A., Frisia, S., Fairchild, I. J., Somogyi, A., & Susini, J. (2007). Trace element distribution in annual stalagmite laminae mapped by micrometer-resolution X-ray fluorescence: Implications for incorporation of environmentally significant species. *Geochimica et Cosmochimica Acta*, *71*(6), 1494–1512. https://doi.org/10.1016/j.gca.2006.12.016

Bowen, G. J. (2025). The online isotopes in precipitation calculator. Retrieved from http://www.waterisotopes.org

Breecker, D. O. (2017). Atmospheric pCO2 control on speleothem stable carbon isotope compositions. *Earth and Planetary Science Letters*, *458*, 58–68. https://doi.org/10.1016/j.epsl.2016.10.042

Breitenbach, S. F. M., Rehfeld, K., Goswami, B., Baldini, J. U., Ridley, H. E., Kennett, D. J., et al. (2012). Constructing proxy records from age models (COPRA). *Climate of the Past*, *8*(5), 1765–1779. https://doi.org/10.5194/cp-8-1765-2012

Bryson, R. A., & Hare, R. K. (1974). The climate of North America. In R. A. Bryson & R. K. Hare (Eds.), *The climate of North America*.

Burns, S. J., Godfrey, L. R., Faina, P., McGee, D., Hardt, B., Ranivoharimanana, L., & Randrianasy, J. (2016). Rapid human-induced landscape transformation in Madagascar at the end of the first millennium of the common era. *Quaternary Science Reviews*, *134*, 92–99. https://doi.org/10.1016/j.quascirev.2016.01.007

Carré, M., Sachs, J. P., Purca, S., Schauer, A. J., Braconnot, P., Falcón, R. A., et al. (2014). Holocene history of ENSO variance and asymmetry in the eastern tropical Pacific. *Science*, *345*(6200), 1045–1048. https://doi.org/10.1126/science.1252220

Chellman, N. J., Pederson, G. T., Lee, C. M., McWethy, D. B., Puseman, K., Stone, J. R., et al. (2021). High elevation ice patch documents Holocene climate variability in the northern Rocky Mountains. *Quaternary Science Advances*, *3*, 100021. https://doi.org/10.1016/j.qsa.2020.100021

Cole, J. E., & Cook, E. R. (1998). The changing relationship between ENSO variability and moisture balance in the continental United States. *Geophysical Research Letters*, *25*(24), 4529–4532. https://doi.org/10.1029/1998GL900145

Conroy, J. L., Overpeck, J. T., Cole, J. E., Shanahan, T. M., & Steinitz-Kannan, M. (2008). Holocene changes in eastern tropical Pacific climate inferred from a Galápagos lake sediment record. *Quaternary Science Reviews*, *27*(11–12), 1166–1180. https://doi.org/10.1016/j.quascirev.2008.02.015

Cook, B. I., Cook, E. R., Smerdon, J. E., Seager, R., Williams, A. P., Coats, S., et al. (2016). North American megadroughts in the common era: Reconstructions and simulations. *Wiley Interdisciplinary Reviews: Climate Change*, *7*(3), 411–432. https://doi.org/10.1002/wcc.394

Cook, E. R., Seager, R., Cane, M. A., & Stahle, D. W. (2007). North American drought: Reconstructions, causes, and consequences. *Earth-Science Reviews*, *81*(1–2), 93–134. https://doi.org/10.1016/j.earscirev.2006.12.002

D'Arrigo, R., Villalba, R., & Wiles, G. (2001). Tree-ring estimates of Pacific decadal climate variability. *Climate Dynamics*, *18*(3), 219–224. https://doi.org/10.1007/s003820100177

Dettinger, M. D., Cayan, D. R., Diaz, H. F., & Meko, D. M. (1998). North–south precipitation patterns in western North America on interannual-to-decadal timescales. *Journal of Climate*, *11*(12), 3095–3111. https://doi.org/10.1175/1520-0442(1998)011<3095:NSPPIW>2.0.CO;2

Ersek, V., Clark, P. U., Mix, A. C., Cheng, H., & Edwards, R. L. (2012). Holocene winter climate variability in mid-latitude western North America. *Nature Communications*, *3*(1), 1–8. https://doi.org/10.1038/ncomms2222

Fisler, J., & Hendy, I. L. (2008). California current system response to late Holocene climate cooling in southern California. *Geophysical Research Letters*, *35*(9), L09702. https://doi.org/10.1029/2008GL033902

Fohlmeister, J., Voarintsoa, N. R. G., Lechleitner, F. A., Boyd, M., Brandtstätter, S., Jacobson, M. J., & Oster, J. L. (2020). Main controls on the stable carbon isotope composition of speleothems. *Geochimica et Cosmochimica Acta*, *279*, 67–87. https://doi.org/10.1016/j.gca.2020.03.042

Giamalaki, K., Beaulieu, C., Henson, S. A., Martin, A. P., Kassem, H., & Faranda, D. (2021). Future intensification of extreme Aleutian low events and their climate impacts. *Scientific Reports*, *11*(1), 18395. https://doi.org/10.1038/s41598-021-97615-7

Hunter, T., Tootle, G., & Piechota, T. (2006). Oceanic-atmospheric variability and western US snowfall. *Geophysical Research Letters*, *33*(13), L13706. https://doi.org/10.1029/2006GL026600

Jiménez-Moreno, G., Anderson, R. S., & Shinker, J. J. (2021). ENSO, sun and megadroughts in SW USA during the last 11,000 years. *Earth and Planetary Science Letters*, *576*, 117217. https://doi.org/10.1016/j.epsl.2021.117217

Koutavas, A., Demenocal, P. B., Olive, G. C., & Lynch-Stieglitz, J. (2006). Mid-holocene El Niño–Southern oscillation (ENSO) attenuation revealed by individual Foraminifera in eastern tropical Pacific sediments. *Geology*, *34*(12), 993–996. https://doi.org/10.1130/G22810A.1

Koutavas, A., & Joanides, S. (2012). El Niño–Southern oscillation extrema in the Holocene and last glacial maximum. *Paleoceanography*, *27*(4). https://doi.org/10.1029/2012pa002378

Lachniet, M. S., Denniston, R. F., Asmerom, Y., & Polyak, V. J. (2014). Orbital control of western North America atmospheric circulation and climate over two glacial cycles. *Nature Communications*, *5*(1), 1–8. https://doi.org/10.1016/B978-0-444-63590-7.00020-2

Ladd, M., Viau, A. E., Way, R. G., Gajewski, K., & Sawada, M. C. (2018). Variations in precipitation in North America during the past 2000 years. *The Holocene*, *28*(4), 667–675. https://doi.org/10.1177/0959683617735583

Larsen, D. J., Crump, S. E., & Blumm, A. (2020). Alpine glacier resilience and Neoglacial fluctuations linked to Holocene snowfall trends in the western United States. *Science Advances*, *6*(47), eabc7661. https://doi.org/10.1126/sciadv.abc7661

Lehmann, S. B., Steinman, B. A., Finkenbinder, M. S., & Abbott, M. B. (2021). Prolonged early to middle Holocene drought in the Pacific Northwest inferred from lacustrine carbonate oxygen isotope values and sedimentology. *Quaternary Science Reviews*, *271*, 107192. https://doi.org/10.1016/j.quascirev.2021.107192

Liefert, D. T., & Shuman, B. N. (2022). Expression of the "4.2 ka event" in the southern rocky Mountains, USA. *Climate of the Past*, *18*(5), 1109–1124. https://doi.org/10.5194/cp-18-1109-2022

Lundeen, Z., Brunelle, A., Burns, S. J., Polyak, V., & Asmerom, Y. (2013). A speleothem record of Holocene paleoclimate from the northern Wasatch Mountains, southeast Idaho, USA. *Quaternary International*, *310*, 83–95. https://doi.org/10.1016/j.quaint.2013.03.018

Malloy, K. M., & Kirtman, B. P. (2020). Predictability of midsummer Great Plains low-level jet and associated precipitation. *Weather and Forecasting*, *35*(1), 215–235. https://doi.org/10.1175/waf-d-19-0103.1

Mark, S., Whitlock, C., Abbott, M., Steinman, B., Fernandez, A., & Steeple, J. (2024). The influence of multidecadal climate variability and abrupt landscape change on terrestrial ecosystem composition and fire regime in the upper Columbia River basin-A high-resolution Holocene perspective. *Quaternary Science Reviews*, *333*, 108668. https://doi.org/10.1016/j.quascirev.2024.108668

Mark, S. Z., Abbott, M. B., Rodbell, D. T., & Moy, C. M. (2022). XRF analysis of Laguna Pallcacocha sediments yields new insights into Holocene El Niño development. *Earth and Planetary Science Letters*, *593*, 117657. https://doi.org/10.1016/j.epsl.2022.117657

Mickler, P. J., Stern, L. A., & Banner, J. L. (2006). Large kinetic isotope effects in modern speleothems. *Geological Society of America Bulletin*, *118*(1–2), 65–81. https://doi.org/10.1130/B25698.1

Nagashima, K., Addison, J., Irino, T., Omori, T., Yoshimura, K., & Harada, N. (2021). Aleutian Low variability for the last 7500 years and its relation to the westerly Jet. *Quaternary Research*, *108*, 1–19. https://doi.org/10.1017/qua.2020.116

Oster, J. L., Montañez, I. P., & Kelley, N. P. (2012). Response of a modern cave system to large seasonal precipitation variability. *Geochimica et Cosmochimica Acta*, *91*, 92–108. https://doi.org/10.1016/j.gca.2012.05.027

Oster, J. L., Weisman, I. E., & Sharp, W. D. (2020). Multi-proxy stalagmite records from northern California reveal dynamic patterns of regional hydroclimate over the last glacial cycle. *Quaternary Science Reviews*, *241*, 106411. https://doi.org/10.1016/j.quascirev.2020.106411

Parvez, Z. A., El-Shenawy, M. I., Lucarelli, J. K., Kim, S. T., Johnson, K. R., Wright, K., et al. (2024). Dual carbonate clumped isotope (Δ47-Δ48) measurements constrain different sources of kinetic isotope effects and quasi-equilibrium signatures in cave carbonates. *Geochimica et Cosmochimica Acta*, *366*, 95–112. https://doi.org/10.1016/j.gca.2023.11.017

Pederson, G. T., Gray, S. T., Woodhouse, C. A., Betancourt, J. L., Fagre, D. B., Littell, J. S., et al. (2011). The unusual nature of recent snowpack declines in the North American Cordillera. *Science*, *333*(6040), 332–335. https://doi.org/10.1126/science.1201570

Praetorius, S. K., Mix, A. C., Walczak, M. H., Wolhowe, M. D., Addison, J. A., & Prahl, F. G. (2015). North Pacific deglacial hypoxic events linked to abrupt ocean warming. *Nature*, *527*(7578), 362–366. https://doi.org/10.1038/nature15753

Preece, J. R., Shinker, J. J., Riebe, C. S., & Minckley, T. A. (2020). Elevation-dependent precipitation response to El Niño-Southern oscillation revealed in headwater basins of the US central Rocky Mountains. *International Journal of Climatology*, *41*(2), 1199–1210. https://doi.org/10.1002/joc.6790

Pribyl, P., & Shuman, B. (2014). A computational method for lake-level reconstruction applied in the central Rocky Mountains, USA. *Quaternary Research*, *82*(1), 249–259. https://doi.org/10.1016/j.yqres.2014.01.012

Reschke, M., Kunz, T., & Laepple, T. (2019). Comparing methods for analysing time scale dependent correlations in irregularly sampled time series data. *Computational Geosciences*, *123*, 65–72. https://doi.org/10.1016/j.cageo.2018.11.009

Rodysill, J. R., Russell, J. M., Vuille, M., Dee, S., Lunghino, B., & Bijaksana, S. (2019). La Niña-driven flooding in the Indo-Pacific warm pool during the past millennium. *Quaternary Science Reviews*, *225*, 106020. https://doi.org/10.1016/j.quascirev.2019.106020

Shinker, J. J., & Bartlein, P. J. (2009). Visualizing the large-scale patterns of ENSO-related climate anomalies in North America. *Earth Interactions*, *13*(3), 1–50. https://doi.org/10.1175/2008ei244.1

Shuman, B. N., Pribyl, P., & Buettner, J. (2015). Hydrologic changes in Colorado during the mid-Holocene and Younger Dryas. *Quaternary Research*, *84*(2), 187–199. https://doi.org/10.1016/j.yqres.2015.07.004

Shuman, B. N., Routson, C., McKay, N., Fritz, S., Kaufman, D., Kirby, M. E., et al. (2018). Placing the common Era in a Holocene context: Millennial to centennial patterns and trends in the hydroclimate of North America over the past 2000 years. *Climate of the Past*, *14*(5), 665–686. https://doi.org/10.5194/cp-14-665-2018

Shuman, B. N., & Serravezza, M. (2017). Patterns of hydroclimatic change in the Rocky Mountains and surrounding regions since the last glacial maximum. *Quaternary Science Reviews*, *173*, 58–77. https://doi.org/10.1016/j.quascirev.2017.08.012

Sinclair, D. J., Banner, J. L., Taylor, F. W., Partin, J., Jenson, J., Mylroie, J., et al. (2012). Magnesium and strontium systematics in tropical speleothems from the Western Pacific. *Chemical Geology*, *294*, 1–17. https://doi.org/10.1016/j.chemgeo.2011.10.008

Sjostrom, D. J., Hren, M. T., Horton, T. W., Waldbauer, J. R., & Chamberlain, C. P. (2006). Stable isotopic evidence for a pre–late Miocene elevation gradient in the Great Plains–Rocky Mountain region. *Geological Society of America Special Papers*, *398*, 309–319. https://doi.org/10.1130/2006.2398

Skiba, V., & Fohlmeister, J. (2023). Contemporaneously growing speleothems and their value to decipher in-cave processes–A modelling approach. *Geochimica et Cosmochimica Acta*, *348*, 381–396. https://doi.org/10.1016/j.gca.2023.03.016

Steinman, B. A., Abbott, M. B., Mann, M. E., Ortiz, J. D., Feng, S., Pompeani, D. P., et al. (2014). Ocean-atmosphere forcing of centennial hydroclimate variability in the Pacific Northwest. *Geophysical Research Letters*, *41*(7), 2553–2560. https://doi.org/10.1002/2014gl059499

Steinman, B. A., Abbott, M. B., Mann, M. E., Stansell, N. D., & Finney, B. P. (2012). 1,500 year quantitative reconstruction of winter precipitation in the Pacific Northwest. *Proceedings of the National Academy of Sciences*, *109*(29), 11619–11623. https://doi.org/10.1073/pnas.1201083109

Stone, L., Strong, C., Bai, H., Reichler, T., McCabe, G., & Brooks, P. D. (2023). Atlantic-Pacific influence on western US hydroclimate and water resources. *npj Climate and Atmospheric Science*, *6*(1), 139. https://doi.org/10.1038/s41612-023-00471-7

Sung, M. K., An, S. I., Kim, B. M., & Woo, S. H. (2014). A physical mechanism of the precipitation dipole in the western United States based on PDO-storm track relationship. *Geophysical Research Letters*, *41*(13), 4719–4726. https://doi.org/10.1002/2014GL060711

Thirumalai, K., DiNezio, P. N., Partin, J. W., Liu, D., Costa, K., & Jacobel, A. (2024). Future increase in extreme El Niño supported by past glacial changes. *Nature*, *634*(8033), 374–380. https://doi.org/10.1038/s41586-024-07984-y

Tremaine, D. M., & Froelich, P. N. (2013). Speleothem trace element signatures: A hydrologic geochemical study of modern cave dripwaters and farmed calcite. *Geochimica et Cosmochimica Acta*, *121*, 522–545. https://doi.org/10.1016/j.gca.2013.07.026

Wilson, R., Wiles, G., D'Arrigo, R., & Zweck, C. (2007). Cycles and shifts: 1,300 years of multi-decadal temperature variability in the Gulf of Alaska. *Climate Dynamics*, *28*(4), 425–440. https://doi.org/10.1007/s00382-006-0194-9

Wise, E. K. (2010). Spatiotemporal variability of the precipitation dipole transition zone in the western United States. *Geophysical Research Letters*, *37*(7), L07706. https://doi.org/10.1029/2009GL042193

Wise, E. K. (2016). Five centuries of US West Coast drought: Occurrence, spatial distribution, and associated atmospheric circulation patterns. *Geophysical Research Letters*, *43*(9), 4539–4546. https://doi.org/10.1002/2016GL068487

Woodhouse, C. A., Russell, J. L., & Cook, E. R. (2009). Two modes of North American drought from instrumental and paleoclimatic data. *Journal of Climate*, *22*(16), 4336–4347. https://doi.org/10.1175/2009JCLI2705.1

References From the Supporting Information

Bowen, G. J., Wassenaar, L. I., & Hobson, K. A. (2005). Global application of stable hydrogen and oxygen isotopes to wildlife forensics. *Oecologia*, *143*(3), 337–348. https://doi.org/10.1007/s00442-004-1813-y

Cheng, H., Edwards, R. L., Shen, C. C., Polyak, V. J., Asmerom, Y., Woodhead, J., et al. (2013). Improvements in 230Th dating, 230Th and 234U half-life values, and U–Th isotopic measurements by multi-collector inductively coupled plasma mass spectrometry. *Earth and Planetary Science Letters*, *371*, 82–91. https://doi.org/10.1016/j.epsl.2013.04.006

Daly, C. (2002). *Variable influence of terrain on precipitation patterns: Delineation and use of effective terrain height in PRISM* (Vol. 7). Oregon State University.

Despain, D. G. (1987). The two climates of Yellowstone national Park. *Proceedings of the Montana Academy of Science*, *47*, 11–20.

Edwards, R. L., Chen, J. H., & Wasserburg, G. J. (1987). 238U 234U 230Th 232Th systematics and the precise measurement of time over the past 500,000 years. *Earth and Planetary Science Letters*, *81*(2–3), 175–192. https://doi.org/10.1016/0012-821X(87)90154-3

Holden, N. E. (1989). Total and spontaneous fission half-lives for uranium, plutonium, americium and curium nuclides. *Pure and Applied Chemistry*, *61*(8), 1483–1504. https://doi.org/10.1351/pac198961081483

Jaffey, A. H., Flynn, K. F., Glendenin, L. E., Bentley, W. T., & Essling, A. M. (1971). Precision measurement of half-lives and specific activities of U 235 and U 238. *Physical Review C*, *4*(5), 1889–1906. https://doi.org/10.1103/PhysRevC.4.1889

Knowles, N., Dettinger, M. D., & Cayan, D. R. (2006). Trends in snowfall versus rainfall in the western United States. *Journal of Climate*, *19*(18), 4545–4559. https://doi.org/10.1175/jcli3850.1

Kohn, M. J., & McKay, M. (2010). Stable isotopes of fossil teeth corroborate key general circulation model predictions for the last glacial Maximum in North America. *Geophysical Research Letters*, *37*(22). https://doi.org/10.1016/j.palaeo.2012.01.037

Kohn, M. J., & McKay, M. P. (2012). Paleoecology of late Pleistocene–Holocene faunas of eastern and central Wyoming, USA, with implications for LGM climate models. *Palaeogeography, Palaeoclimatology, Palaeoecology*, *326*, 42–53. https://doi.org/10.1016/j.palaeo.2012.01.037

Lê, S., Josse, J., & Husson, F. (2008). FactoMineR: An R package for multivariate analysis. *Journal of Statistical Software*, *25*, 1–18. https://doi.org/10.18637/jss.v025.i01

Nelson, D. B., Abbott, M. B., Steinman, B., Polissar, P. J., Stansell, N. D., Ortiz, J. D., et al. (2011). Drought variability in the Pacific Northwest from a 6,000-yr lake sediment record. *Proceedings of the National Academy of Sciences*, *108*(10), 3870–3875. https://doi.org/10.1073/pnas.1009194108

Meachen, J. A., Brannick, A. L., & Fry, T. J. (2016). Extinct Beringian wolf morphotype found in the continental US has implications for wolf migration and evolution. *Ecology and Evolution*, *6*(10), 3430–3438. https://doi.org/10.1002/ece3.2141

Sandberg, C. A., & Klapper, G. (1967). *Stratigraphy, age, and paleotectonic significance of the Cottonwood Canyon member of the Madison limestone in Wyoming and Montana* (pp. B1–B70). US Government Printing Office.

Schoenemann, S. W., Martin, J. T., Pederson, G. T., & McWethy, D. B. (2020). 2,200-year tree-ring and lake-sediment based snowpack reconstruction for the northern Rocky Mountains highlights the historic magnitude of recent snow drought. *Quaternary Science Advances*, *2*, 100013. https://doi.org/10.1016/j.qsa.2020.100013

Shapley, M. D., Ito, E., & Donovan, J. J. (2009). Lateglacial and Holocene hydroclimate inferred from a groundwater flow-through lake, Northern Rocky Mountains, USA. *The Holocene*, *19*(4), 523–535. https://doi.org/10.1177/0959683609104029

Steinman, B. A., Pompeani, D. P., Abbott, M. B., Ortiz, J. D., Stansell, N. D., Finkenbinder, M. S., et al. (2016). Oxygen isotope records of Holocene climate variability in the Pacific Northwest. *Quaternary Science Reviews*, *142*, 40–60. https://doi.org/10.1016/j.quascirev.2016.04.012

Whitlock, C., Dean, W. E., Fritz, S. C., Stevens, L. R., Stone, J. R., Power, M. J., et al. (2012). Holocene seasonal variability inferred from multiple proxy records from Crevice Lake, Yellowstone National Park, USA. *Palaeogeography, Palaeoclimatology, Palaeoecology*, *331*, 90–103. https://doi.org/10.1016/j.palaeo.2012.03.001